# Thermal neutron flux evaluation by a single crystal CVD diamond detector in LHD deuterium experiment


| | |
|---|---|
| journal or publication title | Journal of Instrumentation |
| volume | 14 |
| number | September 2019 |
| year | 2019-09-23 |
| URL | http://hdl.handle.net/10655/00012742 |

doi: 10.1088/1748-0221/14/09/C09039

Creative Commons : 表示
http://creativecommons.org/licenses/by/3.0/deed.ja


# Thermal neutron flux evaluation by a single crystal CVD diamond detector in LHD deuterium experiment

**Makoto Kobayashi[a,b], Kunihiro Ogawa[a,b], Mitsutaka Isobe[a,b], Takeo Nishitani[a], Shuji Kamio[a], Yutaka Fujiwara[a], Tomomi Tsubouchi[c,b], Sachiko Yoshihashi[d], Akira Uritani[d], Minoru Sakama[e], Masaki Osakabe[a,b], and the LHD Experiment Group[a]**

[a]*National Institute for Fusion Science, National Institutes of Natural Sciences, 322-6 Oroshi, Toki, Gifu, Japan.*
[b]*SOKENDAI (Graduate University for Advanced Studies), 322-6 Oroshi, Toki, Gifu, Japan.*
[c]*National Institute for Basic Biology, National Institutes of Natural Sciences, 38 Nishigonaka, Myodaiji, Okazaki, Aichi, Japan.*
[d]*Nagoya University, Furo-cho, Chikusa-ku, Nagoya, Aichi, Japan*
[e]*Tokushima University 2-24, Shinkura-cho, Tokushima, Japan.*

*E-mail*: kobayashi.makoto@nifs.ac.jp

ABSTRACT: A single crystal CVD diamond detector (SDD) was installed in the torus hall of the Large Helical Device (LHD) to measure neutron during deuterium plasma operation. The LiF foil with 95.62 % of $^{6}$Li isotope enrichment pasted on the detector was used as the thermal neutron convertor. The energetic ions of 2.0 MeV alpha and 2.7 MeV triton particles generated by the nuclear reaction of neutron with $^{6}$Li in LiF foil. Then, energetic ions deposited the energy into diamond, producing a signals in SDD.

SDD were exposed to the neutron field in the torus hall of the LHD during the 2nd campaign of the deuterium experiment. The total charge in SDD during one plasma shot in LHD was linearly propotional to the neutron yield over 4 orders of magnitude. The energetic alpha and triton were separately measured by SDD with LiF with the thickness of 1.9 μm, although SDD with LiF with the thickness of 350 μm showed a broadened peak due to the large energy loss of energetic particles generated in the bulk of LiF. The modeling with MCNP and PHITS codes well interpreted the pulse height spectra for SDD with LiF with different thicknesses.

KEYWORDS: diamond detector; neutron; MCNP; PHITS.

## Contents



## 1. Introduction

In the fusion experimental devices using deuterium and/or tritium plasma, high density and high temperature plasma produces a high neutron flux [1-3]. Therefore, the detector measureable for the fast neutron in the radiation background environment is desired for the diagnostics of fusion plasma. Also, the neutron activation in the components in the torus hall is one of the issues from the point of view of safety. Radioactive isotopes emit radiation such as gamma-ray, thus restricting the maintenance work due to the occupational radiation exposure for workers. The cross-sections of activation reactions between neutron and elements in the components largely depend on the neutron energy. Therefore, the advanced neutron detector capable of discriminatively measuring fast, epithermal, thermal neutrons as well as gamma-ray can accelerate physics research and secure radiation safety in the experiment.

For these requirements, one of the solutions is to adopt the single crystal diamond (SCD) [4-10]. The SCD is one of the semiconductor materials. The energy deposited from the radiation into SCD creates the hole-electron pairs. By the bias voltage applied on each surface of SCD, the hole-electron pairs oppositely penetrate through the bulk of SCD. Therefore, one can evaluate the radiation dose as the current which was carried by the hole-electron motion. The single crystal diamond detector (SDD) has advantages such as the tolerance for radiation dose, the high operation temperature, small size, and fast neutron measurement capability [11]. In addition, the pasting of foils consisting of lithium or boron on the SCD can provide SDD with the ability for the measurement of thermal and epithermal neutrons [12]. The energetic ions generated by the nuclear reactions of thermal and epithermal neutrons with lithium and boron such as $^{6}Li(n,\alpha)^{3}H$ and $^{10}B(n,\alpha)^{7}Li$ reactions, respectively, have large energies around 1 MeV or more [13]. Then, the incident energetic ions transfer their energy into SCD. Therefore, the measurement of thermal and epithermal neutrons can be implemented.

The Large Helical Device (LHD) is one of the largest superconducting fusion experimental devices. The deuterium experiments in LHD began in 2017 to obtain the high-performance plasma in helical type fusion device [14-16]. Side by side with physics research, the large volume of the LHD and its torus hall can provide a wide range of neutron flux with various neutron energies, which are available for the other research fields such as medical and biology research.

Therefore, an SDD was installed into the torus hall of LHD in the 2nd campaign of the deuterium experiment. The lithium fluoride (LiF) foil was used as the thermal neutron convertor. The signals from SDD were processed into the pulse height spectrum (PHS) to evaluate the performance of SDD for the measurement of energetic ions.

## 2. Single crystal CVD diamond detector

The SDD used in this study was purchased from Cividec instrumentation GmbH. The SCD was fabricated by the chemical vapor deposition (CVD). The size of the SCD is 4.5 mm × 4.5 mm, and the thickness is 140 μm. The contact titanium electrode is pasted on both sides of SCD. The SCD is in housing with the size of 54 mm × 10 mm × 8 mm made of $Al_2O_3$. There is a window with the diameter of 2.5 mm in the housing in front of one side of the SCD. The lid of the window is the size of 54 mm × 10 mm × 1 mm. The LiF foil is pasted on a surface of the lid. The diamter of the LiF foil is 4 mm, which is sufficiently larger than that of the window in the housing. LiF foil was synthesized with the isotope enrichment of $^6$Li as 95.62 % to increase the sensitivity for thermal neutron. In the measurement, a side of the lid with the LiF foil faced to the SCD through the window in the housing so that the energetic ions generated in the foil can implant into the SCD directly. The distance between the LiF foil and SCD is 1 mm. The picture of the SDD and the lid is shown in Fig. 1. In this study, two types of LiF foil with different thicknesses as 1.9 μm and 350 μm were used to evaluate the influence of energy loss of energetic ions in the LiF foils on the SDD signal. In the case of 350 μm-thick LiF, the lid was taken apart from the SDD, and the LiF was put on the window of SDD.

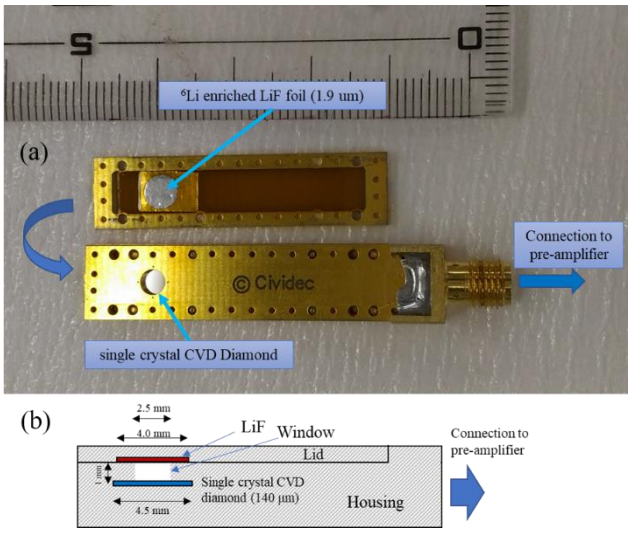


**Figure 1**. (a) the picutre of SDD with the lid pasted with 1.9 μm LiF, (b) the schematic view of the cross-section of SDD

In the measurement, SDD was sealed into the ICF-34 metal flange to reduce the tritium release. Then, bias voltage of -120 V was applied to a surface of the SDD through the pre-amplifier (HV broadband Amplifier) of Cividec instrumentation GmbH. The signal from SDD was acquired by fast processing ADC and FPGA. The sampling rate of this system was 1 GHz.

## 3. Particle transport modeling

The count rate of energtic ions (alpha and triton) by the SDD depends not only on the neutron flux and neutron energy, but also on the transport processes of energetic ions in the LiF foil. Therefore, the neutron tranport in the torus hall and the secondary energetic ion transport in the SDD must be calculated. In this study, MCNP6 (General Mote Carlo N-Particle code) was applied for the neutron transport calculation in the LHD torus hall [17]. Then, the transport processes of energetic ions in SDD, including generation, energy loss in LiF foil, and energy deposition into SCD, were calculated by PHITS (Particle and Heavy Ion Transport code System) [18].

The neutron transport model for MCNP6 calculation has been developed for LHD [19]. The model includes the torus hall, LHD body, coils, support structure. With the track-lengh estimation tally of MCNP6, the neutron energy spectrum at the position of SDD could be evaluated.

The transport calculation for energetic ions was conducted by PHITS with using the neutron energy spectrum evaluated by MCNP6 calculation. For the calculation in PHITS, the SDD was carefully modeled. Then, two plane neutron sources were set at the opposite direction to the SDD. The size of the plane neutron source was 5 mm ×5 mm, which is sufficiently larger than that of SCD and LiF foil. These neutron sources have the same neutron energy spectrum evaluated by MCNP6 calculation. The event generator mode was applied to precisely evaluate the energy and the momentum of energetic ions generated by the nuclear reaction. The averaged count as a function of deposited energy into SCD in a single event was estimated by T-deposit tally, which is a track-lenght estimation tally in PHITS. For this tally, the statistical dispersion on the deposited energy was set to be a gaussian distribution. Also, the trigger level was imitated by setting the cut-off energy of around 300 keV.

## 4. Neutron irradiation in the torus hall of LHD

The deuterium plasma induces two branching fusion reaction of $^{2}H(d,p)^{3}H$ and $^{2}H(d,n)^{3}He$. The cross-sections for these reactions are almost the same. The latter reaction produces neutron with the energy of 2.45 MeV. The former reaction produces triton. A part of triton generated in the plasma subsequently reacts with deuteron with $^{3}H(d,n)^{4}He$ reaction which emits the 14.1 MeV neutron. This reaction is called a triton burn-up reaction, and 0.05-0.4 % of triton induces this reaction in a plasma operation [20,21]. Consequently, neutrons originated from 2.45 MeV (dominant) and 14.1 MeV (minor) are transported in the torus hall.

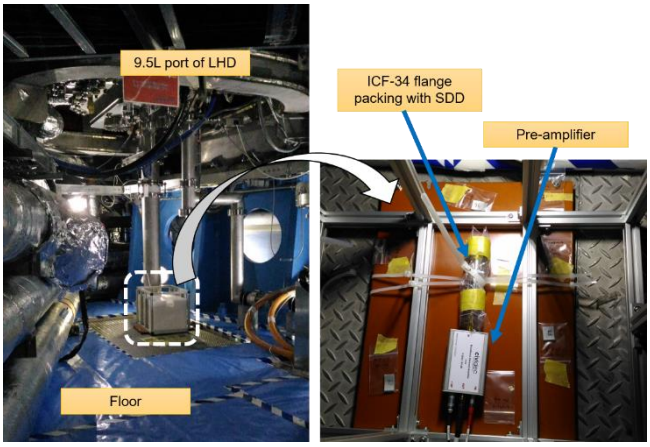


**Figure 2.** Picture of SDD set underneath 9.5L port of LHD in the torus hall.

The SDD was installed into the torus hall of LHD. The position of SDD was underneath the 9.5L port of LHD, and placed near the floor level, corresponding to the distance of 5.5 m from the plasma. The picture of SDD in the torus hall of LHD is shown in Fig. 2. The signal from the SDD was transferred to the DAQ system in the basement of the torus hall. The binary file made from the measurement data was processed by the python numpy module.

The signal from the SDD was obtained in each plasma operation (shot) in LHD. The total charge in a single event (the area of a pulse) corresponds to the deposited energy from a particle. PHS was acquired by the histogram of the total charge. The neutron yield was different in each plasma shot, and monitored by the neutron flux monitor (NFM). The SDD with the 1.9 μm-thick LiF foil was exposed to neutron in the plasma shot number of #147425-#147820. That with 350 μm-thick LiF foil was placed in the torus hall during the plasma shot number of #147886-#148459.

## 5. Results and discussion

Fig. 3 shows ten typical signals from SDD with 1.9 μm-thick LiF during deuterium plasma shot. The individual pulse durations were within about 10 ns. The shapes of the signal were almost the same for SDD with LiF with the thicknesses of 1.9 and 350 μm. The signals can be separated into large pulse and small pulse. In the nuclear reaction of $^{6}Li(n,\alpha)^{3}H$, the recoil energies of alpha and triton particles are around 2.0 MeV and 2.7 MeV, respectively. Also, these particles recoil in the opposite direction of each other. Hence, when either particle injects into SCD, another particle implants into the lid of SDD. Consequently, the large pulse should correspond to the deposition of triton. The small pulse would be caused by alpha particle.

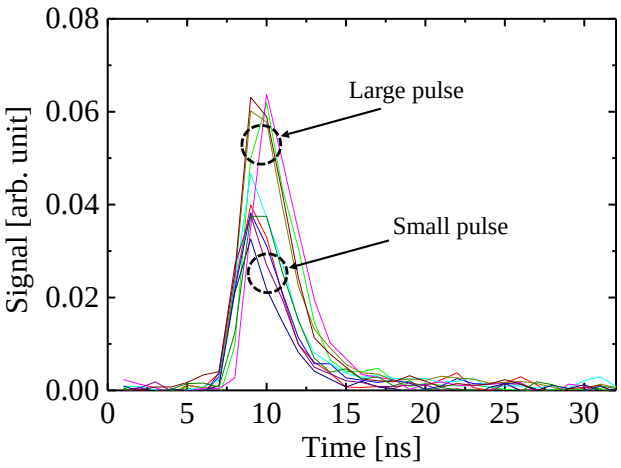


**Figure 3.** Typical signals from SDD with 1.9 μm-thick LiF

The correlation between the total charge in SDD and the neutron yield in each plasma shot are summarized in Fig. 4. The linear relationship between the total charge and the neutron yield in the wide neutron yield ranging from $10^{12}$-$10^{16}$ n/shot was obtained. This result indicates that the counting loss of SDD was quite small in this experimental condition. The total charge in SDD with 350 μm-thick LiF was almost 3.6 times as large as that with LiF with the thickness of 1.9 μm. Compared with thinner LiF foil, the thicker LiF foil can produce more energetic ions, even larger energy loss of energetic ions in the foil, resuling in the higher count rate in SDD.

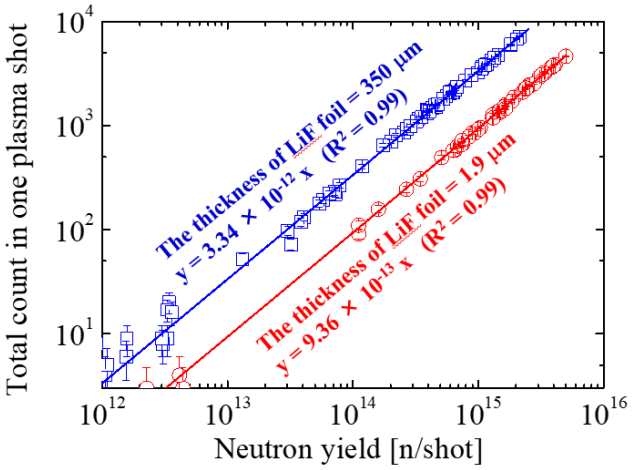


**Figure 4.** Correlation between the total charge in SDD and neutron yield in each plasma shot

The PHS for SDD with 1.9 μm-thick LiF and 350 μm-thick LiF are shown in Fig. 5. Note that the count in perpendicular axis in Fig. 5 is normalized by the neutron yield. A broadend peak was found in the case with 350 μm-thick LiF. Besides, in the case with 1.9 μm-thick LiF, two peaks were observed. According to Fig. 3, the peak appeared in lower energy side was assigned to alpha particle. The peak in the higher energy side was attributed to triton. Also, the peak areas for triton was two times larger than that by alpha particle even though the same number of alpha and triton generated in the LiF foil. This difference could be caused by the energy loss efficiency of these energetic ions in the LiF foil.

The PHS estimated by PHITS code in the cases for SDD with 1.9 μm-thick LiF and 350 μm-thick LiF are shown in Figs. 6 (a) and (b), respectively. Compared with Fig. 5, PHITS code sucessfully reproduced the PHS for these two cases observed in the experiment. The peak areas

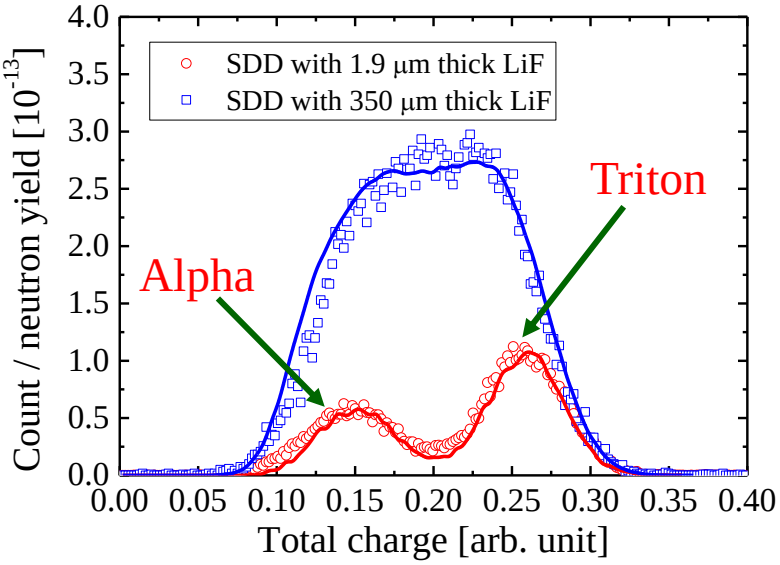


**Figure 5**. PHS for SDD with LiF with different thicknesses. The solid lines in each case are the PHS spectra of energetic particles (alpha + triton) evaluated by PHITS as same as Fig. 6.

in the case with 350 μm-thick LiF was about 3.5 times as large as that in the case with 1.9 μm-thick LiF foil. This is consistent with the difference in the relation of total charge and the neutron yield in each shot for SDD with different thicknesses of LiF as shown in Fig. 4.

The peak position of triton in Fig. 6 (a) was located at 2.7 MeV corresponding to the primitive recoil energy of triton in $^{6}Li(n,\alpha)^{3}H$ reaction. However, the peak position for alpha particle was around 1.5 MeV, which is lower than the virgin recoil energy of alpha particle generated in $^{6}Li(n,\alpha)^{3}H$ reaction. In addition, in Fig. 6 (b), the dominant contributing energetic ion on the PHS for SDD is triton. This means that most of alpha particles could not penetrate through the LiF foil with the thickness of 350 μm. These results can be caused by the difference in the energy loss efficiency between 2.0 MeV alpha and 2.7 MeV triton in LiF foil. Because of the larger positive charge and the mass of alpha particle, the energy loss of alpha particle is larger than that of triton. Of course, triton is also influenced by the energy loss process in LiF. Therefore, in Fig. 6 (b), the peak was broadened due to the wide range of the rest of the energy in triton which depends on the depth of LiF where the triton was generated. According to the PHS evaluated by PHITS, one can estimate the thermal neutron flux at the position of the SDD in the torus hall of LHD. Consequently, the thermal neutron flux of $1.0 \times 10^{-8}$ n cm$^{-2}$ s$^{-1}$ for single

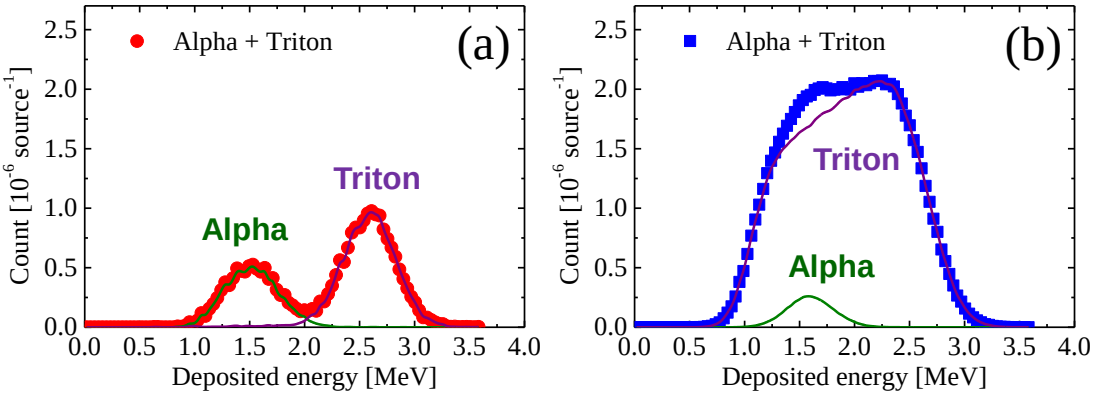


**Figure 6.** The PHS of SDD with (a) 1.9 μm LiF and (b) 350 μm LiF estimated by PHITS.

neutron source was obtained. This value is consistent with our previous research with using activation foil method [22].

The exposure of the SDD with LiF foil to the neutron field in the torus hall of the LHD during deuterium experiment showed the sufficient capability of the measurement for thermal neutron. However, fast neutrons were hardly detected in this work, although the fast neutron detection capability is the typical advantages of SDD. The fast neutron interacts with the diamond by the elastic scattering or the nuclear reaction. For the case fast neutron originated from $^{2}H(d,n)^{3}He$ fusion reaction (2.45 MeV neutron), the elastic scattering is only a channel to interact with diamond. In this process, fast neutron can deposit a part of energy into the diamond up to several hundred keV. However, due to the sufficiently high trigger level in ADC used in this work, the contribution of the elastic scattering by 2.45 MeV neutron in the PHS was excluded.

For the case fast neutron originated from $^{3}H(d,n)^{4}He$ fusion reaction (14.1 MeV neutron), the elastic scattering can deposit the sufficient energy into diamond to be detected. Also, the generation of charged particles in the diamond by $^{12}C(n,\alpha)^{9}Be$ reaction can be another channel to interact with diamond detector. In this process, most of energy of charged particles can transfer into diamond, therefore, a peak in higher energy side should be observed in the PHS spectrum. This reaction requires the threshold neutron energy above 7 MeV [13]. Therefore, only neutrons generated by $^{3}H(d,n)^{4}He$ reaction can overcome this threshold energy. The most possible reason why the signals caused by the nuclear reaction and by the elastic collision were hardly observed in PHS spectrum in this work should be a low flux of 14.1 MeV neutron because of the small triton burn-up ratio in the deuterium plasma . Also, the low cross-section of $^{12}C(n,\alpha)^{9}Be$ reaction [23], a small size of SDD, and the far distance between the SDD and the plasma, are other reasons. The modification of SDD position as well as the enlargement of the SCD size are planned for the next deuterium experiment campaign.

## 6. Conclusion

In this study, a single crystal CVD diamond detector (SDD) was installed into the torus hall of LHD to measure the thermal neutron during plasma operation. The LiF foils affixed to the detector was used as the thermal neutron convertor into the energetic ions of alpha and triton particles. A good linearity between the total charge in SDD and the neutron yield in each plasma operation in LHD was observed. The energetic alpha and triton were separately measured by SDD with LiF with the thickness of 1.9 μm, although SDD with LiF with the thickness of 350 μm showed a broadened peak. The modeling with MCNP and PHITS codes well interpreted the pulse height spectra for SDD with LiF with different thicknesses.

## Acknowledgments

We would like to thank Dr. Erich Griesmayer and Dr. Christina Weiss of CIVIDEC for providing the useful discussion. This work is supported by the NINS program for cross-disciplinary study (Grant Number 0131190), the NIFS Collaboration Research Program (NIFS19KOAA001), and LHD project budget.

## References

[1] M. Ishikawa et al., First measurement of neutron emission profile on JT-60U using Stilbene neutron detector with neutron-gamma discrimination, *Rev. Sci. Instrum.* **73** (2002) 4237.

[2] P.V. Belle et al., Calibration of the JET neutron yield monitors using the delayed neutron counting technique, *Rev. Sci. Instrum.* **61** (1990) 3178.

[3] Z. Stancar et al., Generation of a plasma neutron source for Monte Carlo neutron transport calculations in the tokamak JET, *Fusion Eng. Des.*, **136** (2018) 1047-1051.

[4] C. Cazzaniga et al., Single crystal diamond detector measurements of deuterium-deuterium and deuterium-tritium neutrons in Joint European Torus fusion plasmas, *Rev. Sci. Instrum.* 85, (2014) 043506.

[5] C. Cazzaniga et al., A diamond based neutron spectrometer for diagnostics of deuterium-tritium fusion plasmas, *Rev. Sci. Instrum*. 85, (2014) 11E101.

[6] L. Giacomelli et al., Neutron emission spectroscopy of DT plasmas at enhanced energy resolution with diamond detectors, *Rev.Sci. Instrum*. 87, (2016) 11D822.

[7] D Rigamonti et al., Neutron spectroscopy measurements of 14 MeV neutrons at unprecedented energy resolution and implications for deuterium tritium fusion plasma diagnostics, *Meas. Sci.Technol*, 29 (2018), 4.

[8] M. Nocente et al., Fast ion energy distribution from third harmonic radio frequency heating measured with a single crystal diamond detector at the Joint European Torus, *Rev. Sci. Instrum*. 86, (2015) 103501.

[9] M. Rebai et al., Pixelated Single-crystal Diamond Detector for fast neutron measurements, *J. Instrum*, 10 (2015) C03016.

[10] A. Muraro et al., First neutron spectroscopy measurements with a pixelated diamond detector at JET, Rev. Sci. Instrum. 87, (2016) 11D833.

[11] V.D. Lovalchuk et al., Diamond detector as fast neutron spectrometer, *Nucl. Instrum. Meth. Phys. Res. A*, **351** (1994) 590-591.

[12] S. Alaviva et al., Thermal and fast neutron detection in chemical vapor deposition single-crystal diamond detectors, *Rev. Sci. Instrum.* **103** (2008) 054501.

[13] K. Shibata, et al, JENDL-4.0: A New Library for Nuclear Science and Engineering, *J. Nucl. Sci. Technol*. **48** (2011) 1-30.

[14] Y. Takeiri, The Large Helical Device: entering deuterium experiment phase toward steady-state helical fusion reactor based on achievements in hydrogen experiment phase, *IEEE T. Plasma Sci*., **46** (2018) 2348-2353.

[15] A. Komori, et al., Goal and achievements of Large Helical Device project, *Fusion Sci. Technol*., **58** (2010) 1-11.

[16] Y. Takeiri, et al, Extension of the operational regime of the LHD towards a deuterium experiment, *Nucl. Fusion*, **57** (2017) 102023.

[17] X-5 Monte Carlo Team, MCNP User's Guide - Code Version 6.1.1beta, LA-CP-14-00745 (Los Alamos National Laboratory, Los Alamos, 2014).

[18] T. Sato et al., Features of Particle and Heavy Ion Transport code System (PHITS) version 3.02, *J. Nucl. Sci. Technol.*, **55** (2018) 684-690.

[19] T. Nishitani, et al., Monte Carlo simulation of the neutron measurement for the Large Helical Device deuterium experiments, *Fusion Eng. Des*., **123** (2017) 1020-1024.

[20] N. Pu et al., Initial results of triton burnup study in the Large Helical Device, *Plasma. Fusion. Res.*, **13** (2018) 3402121.

[21] K. Ogawa et al., Energetic-ion confinement studies by using comprehensive neutron diagnostics in the Large Helical Device, accepted to *Nucl. Fusion*.

[22] M. Kobayashi et al., First measurements of thermal neutron distribution in the LHD torus hall generated by deuterium experiments, *Fusion Eng. Des.*, **137** (2018) 191-195.

[23] T. Shimaoka et al., A diamond 14 MeV neutron energy spectrometer with high energy resolution, *Rev. Sci. Instrum.* **87** (2016) 023503.